

Efficient preparation of non-trivial quantum states using the Quantum Approximate Optimization Algorithm

Wen Wei Ho^{1*}, Timothy H. Hsieh^{2,3},

¹ Department of Physics, Harvard University, Cambridge, Massachusetts 02138, USA

² Kavli Institute for Theoretical Physics, University of California, Santa Barbara, California 93106, USA

³ Perimeter Institute for Theoretical Physics, Waterloo, Ontario N2L 2Y5, Canada

*wenweiho@fas.harvard.edu

December 3, 2024

Abstract

We provide an efficient and general route for preparing non-trivial quantum states that are not adiabatically connected to unentangled product states. Our approach is a variant of the ‘Quantum Approximate Optimization Algorithm’ (QAOA) [E. Farhi et al., arXiv:1411.4028] and is experimentally realizable on near-term quantum simulators of synthetic quantum systems. As proof of concept, our approach yields explicit protocols which prepare with perfect fidelities (i) the Greenberger-Horne-Zeilinger (GHZ) state, (ii) a quantum critical state, and (iii) a topologically ordered state, all with $p = L/2$ iterations of the algorithm and physical runtimes T that scale linearly with the system size L , i.e. $T \sim L$. The protocol is additionally able to prepare the ground states of antiferromagnetic Heisenberg chains with very good fidelities. Besides being practically useful, our results also illustrate the utility of QAOA-type circuits as variational wavefunctions for non-trivial states of matter.

Contents

1	Introduction	2
2	Non-trivial quantum states	4
3	Quantum Approximate Optimization Algorithm (QAOA)	4
4	Performance of QAOA to prepare certain nontrivial quantum states	5
4.1	GHZ state	5
4.2	Critical state	7
4.3	Ground state of the Toric code	8
4.4	Ground state of AFM Heisenberg chain	9
5	Conclusion	9
A	Optimal angles for preparing GHZ state at $p = L/2$	10

B	Explicit nonuniform unitary circuit for preparing the GHZ state	11
C	Energy optimization plot and optimal angles for preparing critical state at $p = L/2$	11
D	A Conjecture and Numerical Support	12
E	Numerical verification of preparation of toric code ground state	15
F	Effect of errors on QAOA state preparation	16
	References	16

1 Introduction

Recent experimental advances in designing and controlling well-isolated synthetic quantum systems of many-particles, such as trapped ions [1, 2], cold atoms [3, 4], superconducting qubits [5, 6], etc., have allowed for the study of a plethora of interesting physical phenomena. These include topological order [7–9], phase transitions [10, 11], thermalization [12, 13], and time crystals [14, 15]. Equally exciting is the potential to use these platforms for performing quantum simulations and computation [4, 6, 16], or for speed-ups in quantum metrology precision measurements [17–20]. For such studies and the implementation of quantum information protocols, the preparation of complex quantum many-body states, i.e. those with non-trivial patterns of entanglement that are not adiabatically connected to short-ranged entangled states, is vital. For instance, topological states have long-range, non-local patterns of entanglement, and the Greenberger-Horne-Zeilinger (GHZ) state is an essential resource in quantum many-body metrology measurement proposals and has an entanglement pattern that is many-body in nature [17–20]. Furthermore, measurement-based quantum computing requires highly entangled initial states [21–23]. Therefore, it is important to have generic, explicit, resource-efficient schemes for preparing non-trivial quantum states.

In this paper, we demonstrate that the Quantum Approximate Optimization Algorithm (QAOA) serves as an extremely general, versatile and efficient approach for the preparation of non-trivial quantum states of interest. First introduced by Farhi et al. [24, 25] as a method to find approximate solutions to combinatorial optimization problems which are encoded in the ground states of classical Hamiltonians, the QAOA is essentially a hybrid quantum-classical, ‘bang-bang’ protocol: it starts with an easily preparable initial state, and takes as an input a finite set of angles (or times) with which unitary time evolution by two Hamiltonians is sequentially alternated between. A cost function of the resulting state is then evaluated and optimized, which yields a new set of angles to be implemented. The entire process is iterated and the algorithm terminates when the cost function has been desirably optimized (see Fig. 1).

There are two properties which make the QAOA a promising alternative candidate for state preparation (compared to more conventional methods like the quantum adiabatic algorithm (QAA) [26, 27], see also [28]): (i) Firstly, from the Pontryagin principle in optimal control theory [29–32], it is known that the protocol that optimally prepares a quantum state

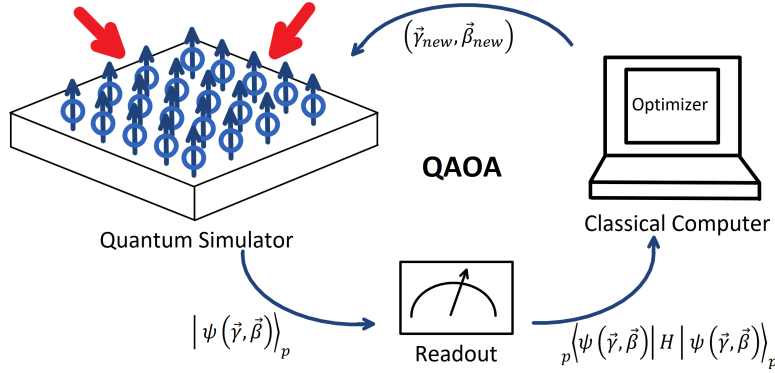


Figure 1: Schematic depiction of the Quantum Approximate Optimization Algorithm and its quantum-classical nature. A quantum simulator of e.g. trapped ions is used to unitarily prepare a target state $|\psi(\gamma, \beta)\rangle_p$ via the QAOA sequence (2) using a set of angles (γ, β) of some fixed number of iterations p . A cost function, for e.g. the global energy ${}_p\langle\psi(\gamma, \beta)|H|\psi(\gamma, \beta)\rangle_p$ is then measured (achievable due to single-site resolution in measurements of quantum simulators). The result is then fed into a classical computer, which finds the next set of angles that optimizes the cost function. The algorithm terminates when the cost function is desirably optimized; the resulting quantum state is then the near to the target state.

within a given time is a ‘bang-bang’ one, where the Hamiltonian is abruptly switched between extremal values within the allowed control parameters. The QAOA, being an example of such a protocol, potentially allows for a more efficient route to prepare nontrivial quantum states. (ii) Secondly, the QAOA is well suited for implementation in current quantum simulators of synthetic quantum systems, leveraging the tunability and single-site resolution of measurements in these platforms. In fact, the feedback loop that is integral to the protocol allows one to mitigate systematic errors that are present in experimental platforms.

As proof of concept, we employ the QAOA to target the GHZ state, the critical state of the 1d transverse field Ising model, and the ground state of the 2d toric code, using simple local Hamiltonians to effect time evolution. We find protocols that remarkably prepare the target states with *perfect fidelities*, all with QAOA protocols of $p = L/2$ iterations, and with minimum runtimes T that scale linearly with the system size, $T \sim L$, where L is the linear dimension of the systems. We also consider preparing the ground states of antiferromagnetic (AFM) Heisenberg chains, and find that the protocol is able to achieve them efficiently and with very good fidelities. This concretely demonstrates the ability of QAOA-type protocols to efficiently and unitarily prepare quantum states with non-trivial patterns of entanglement, and extends its utility beyond the original intention of finding approximate solutions to (classical) combinatorial optimization problems. Note that in the cases of the Ising model and toric code, explicit circuits for the ground states are known, for example in terms of a unitary circuit for the 1d XY-model, exploiting its free fermion nature and fundamentally based on the Fourier transform [33], and in terms of a tensor network representation for the toric code [34]. However, such circuits involve nonuniform applications of multiple types of gates, and are not very practically realizable, especially in analog near-term quantum simulators [35]. This is in contrast to our method, which only requires time evolution between two simple, uniform local Hamiltonians. The QAOA thus provides physically realizable roadmaps for quantum state

preparation.

2 Non-trivial quantum states

Let us start by expounding upon the non-trivial nature of certain quantum states, which we are interested in. Consider a target state $|\psi_t\rangle$ and an unentangled product state $|\psi_u\rangle$, both defined on a system with linear dimension L . $|\psi_t\rangle$ is said to be non-trivial if there does not exist a local unitary circuit U of finite depth (i.e. scaling as $O(L^0)$) that connects the two: $|\psi_t\rangle = U|\psi_u\rangle$ [36]. Instead, the depth of a local unitary circuit connecting the two must be at least $O(L^\alpha)$ with $\alpha > 0$. Intuitively, nontrivial states have entanglement patterns fundamentally different from product states. While this is a statement made at the level of the wavefunction, from the perspective of local Hamiltonians and gaps, such states are separated from product states by a gap-closing phase transition in the thermodynamic limit, and thus preparing them with the QAA is hard.

We now review why the GHZ, critical, and topologically ordered states are nontrivial. Consider first the GHZ state,

$$|\text{GHZ}\rangle \equiv \frac{1}{\sqrt{2}}(\otimes|Z=1\rangle + \otimes|Z=-1\rangle), \quad (1)$$

where X, Z are Pauli operators. Suppose there exists a local, finite-depth unitary U that takes the completely polarized product state $|+\rangle \equiv \otimes|X=1\rangle$ to the GHZ state $|\text{GHZ}\rangle$. Due to locality, there exists a Lieb-Robinson bound which limits the spread of information and entanglement under this evolution, implying that U can only generate a finite correlation length ξ for the final state. Measuring a long-range spin-spin correlator gives $\langle\text{GHZ}|Z_i Z_j|\text{GHZ}\rangle = 1$ while on the other hand the same quantity can be expressed as $\langle+|U^\dagger Z_i U U^\dagger Z_j U|+\rangle$, which in the limit $|i-j| \gg \xi$ decomposes as $\langle+|U^\dagger Z_i U|+\rangle\langle+|U^\dagger Z_j U|+\rangle = \langle\text{GHZ}|Z_i|\text{GHZ}\rangle\langle\text{GHZ}|Z_j|\text{GHZ}\rangle = 0$, a contradiction. Similar arguments apply to critical states which have power-law correlations, and topologically ordered states which have long-range correlations in loop operators and non-zero topological entanglement entropy [37–40].

3 Quantum Approximate Optimization Algorithm (QAOA)

As mentioned, the QAOA begins with an easily prepared state $|\psi_u\rangle$, such as the ground state $|+\rangle$ of a paramagnet $H_X = -\sum_i X_i$. The state is then time evolved by sequentially alternating between two Hamiltonians, for example an interaction Hamiltonian H_I (usually taken to be the Hamiltonian whose ground state we hope to achieve, but this can be tweaked) and the paramagnet H_X for a total of p iterations, so that the resulting state is

$$|\psi(\boldsymbol{\gamma}, \boldsymbol{\beta})\rangle_p = e^{-i\beta_p H_X} e^{-i\gamma_p H_I} \dots e^{-i\beta_1 H_X} e^{-i\gamma_1 H_I} |+\rangle. \quad (2)$$

We call such a protocol QAOA_p . The angles (or times) $(\boldsymbol{\gamma}, \boldsymbol{\beta}) \equiv (\gamma_1, \dots, \gamma_p, \beta_1, \beta_p)$ are to be found by repeatedly optimizing a cost function $F_p(\boldsymbol{\gamma}, \boldsymbol{\beta})$, such as the energy expectation value of the target Hamiltonian:

$$F_p(\boldsymbol{\gamma}, \boldsymbol{\beta}) = {}_p\langle\psi(\boldsymbol{\gamma}, \boldsymbol{\beta})|H_I|\psi(\boldsymbol{\gamma}, \boldsymbol{\beta})\rangle_p, \quad (3)$$

and the state corresponding to these optimal angles is therefore the optimal state that can be prepared by the protocol given this cost function. We note here that it is tempting to view the number of iterations p of the QAOA protocol as the ‘depth’ of a quantum circuit and relate that to its ‘complexity’. However, this is potentially misleading as the QAOA protocol is not a digital quantum circuit comprised of gates drawn from a fixed gate set, but rather depends also on the analog parameters (γ, β) determining the physical runtimes of each Hamiltonian H_I, H_X (see [35] for more details on the difference between digital and analog quantum simulators). As the QAOA is envisioned to be run on near-term quantum simulators which are inherently noisy (so called ‘Noisy, Intermediate-Scale Quantum’ (NISQ) technology), the physical runtimes $t = \sum_i^{p=L/2} (\gamma_i + \beta_i)$ of the QAOA constitute an important measure of the ‘complexity’ or ‘feasibility’ of the algorithm – in general, shorter runtimes lead to less noise encountered and a more successful implementation.

It is clear that the optimal solution from QAOA_{p+1} is always better than QAOA_p ’s. Moreover, for large p the QAOA can approximate the QAA (of the form $H(t) = f(t)H_I + (1 - f(t))H_X$), via Trotterization. Since QAA can achieve with arbitrary accuracy the target ground state of H_I for any finite-size system if the speed of traversal is vanishingly small, this means that the QAOA can also produce with arbitrary accuracy any target ground state in the limit $p \rightarrow \infty$. However, for all practical purposes, the correspondence between the QAOA and QAA at small p is not so clear, and thus in what follows we explore how well the QAOA can target certain hard-to-prepare quantum many-body states beyond those for which it was originally envisioned.

4 Performance of QAOA to prepare certain nontrivial quantum states

We consider using QAOA to prepare the following states: (i) the GHZ state, (ii) a quantum critical ground state, (iii) a topologically ordered state, and (iv) the ground state of an antiferromagnetic (AFM) Heisenberg chain.

4.1 GHZ state

As a first test, we show that this approach can prepare a simple yet nontrivial quantum state, the GHZ state. Consider the $1d$ Ising Hamiltonian

$$H_I = - \sum_{i=1}^L Z_i Z_{i+1} \quad (4)$$

with periodic boundary conditions, for which the GHZ state is the ground state, in symmetry sector $G = \prod_i^L X_i = 1$. If we start with the polarized state $|+\rangle$ which has $G = +1$, then since the QAOA protocol (2) respects this symmetry, optimization of (3) as $p \rightarrow \infty$ will yield the GHZ state, with $\lim_{p \rightarrow \infty} F_p(\gamma, \beta)/L \rightarrow -1$.

We implement the QAOA, finding numerically the optimal angles (γ_*, β_*) that minimize (3) via a search by gradient descent of the parameter space $\gamma_i, \beta_i \in [0, \pi/2)$ for all i , for system sizes $L \leq L_1 = 18$, and for $p \leq L_1/2$. We restrict each angle to be any contiguous interval of length $\pi/2$ because $e^{-i\frac{\pi}{2}H_I} \propto 1$ and $e^{-i\frac{\pi}{2}H_X} \propto G$; furthermore, in order to give the angles (γ, β) an interpretation of ‘time’, we choose $\gamma_i, \beta_i \in [0, \pi/2)$. We note that, for fixed

L , assuming a fine mesh of each interval $[0, \pi/2)$ into \mathcal{M} points, a brute force search of this parameter space takes an exponentially long time $t \sim O(\mathcal{M}^{2p})$ in p . Consequently, we have ensured that the total number of runs performed is large enough to ensure convergence of the search algorithm to the global minimum.

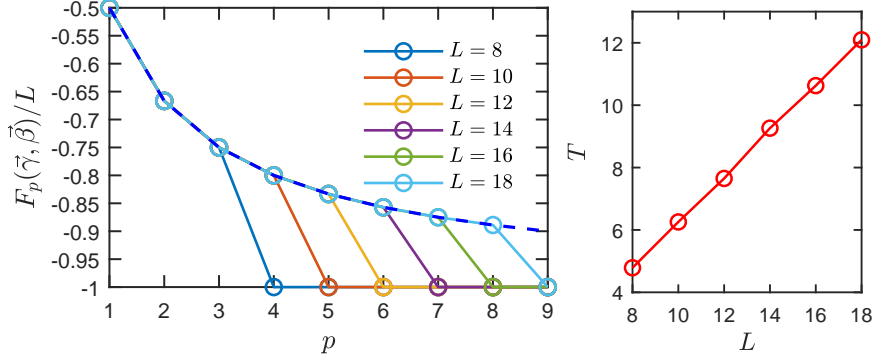


Figure 2: Preparation of GHZ state. (Left) Optimal cost function (3). One sees that $F_p(\gamma, \beta)/L = -1$ for $p \geq L/2$; in other words, the GHZ state is created with perfect fidelity using $\text{QAOA}_{p \geq L/2}$. We have also plotted a conjectured analytic expression $-p/(p+1)$ (from [24]) for the optimal cost function as the dashed blue line. (Right) Total minimum time $T = \min_{(\gamma, \beta)} \left[\sum_{i=1}^{p=L/2} (\gamma_i + \beta_i) \right]$ required for the QAOA to produce the GHZ state with perfect fidelity using $\text{QAOA}_{p=L/2}$. The minimization is performed over all the numerical solutions found. One sees a linear trend $T \sim L$.

Fig. 2 shows the results. We see that interestingly, the GHZ can be prepared with *perfect* fidelity, to machine precision, using the protocol QAOA_{p^*} , with $p^* = L/2$. We note that there are multiple optimal solutions for (γ, β) that give this perfect fidelity (furthermore, the vector of angles is symmetric under the reflection $\gamma_i \leftrightarrow \beta_{L-i+1}$; this is due to the Kramers-Wannier duality of the Ising model which relates the paramagnet (product state) and the ferromagnet (GHZ)). Since each angle γ_i, β_i is bounded from above, our numerical results imply that the time t needed to prepare the GHZ state in a system of size L , using QAOA, is $t = O(L)$. Indeed, in fig. 2, we see that the *minimum* amount of time $T = \min_{(\gamma, \beta)} \left[\sum_{i=1}^{p=L/2} (\gamma_i + \beta_i) \right]$ amongst all the solutions that we numerically found at $p = L/2$, gives an almost perfect linear trend $T \sim L$ (see [41] for the explicit optimal angles).

We remark that various quantum circuits are known to also exactly prepare the GHZ state (for example, using a combination of Hadamard and CNOT gates, see also [41]). Furthermore, experimentally, GHZ states of various sizes have been prepared with high fidelity using the Mølmer-Sørensen technique [42, 43] in trapped ions. Our QAOA protocol is complementary in that it provides a uniform circuit that achieves the same result.

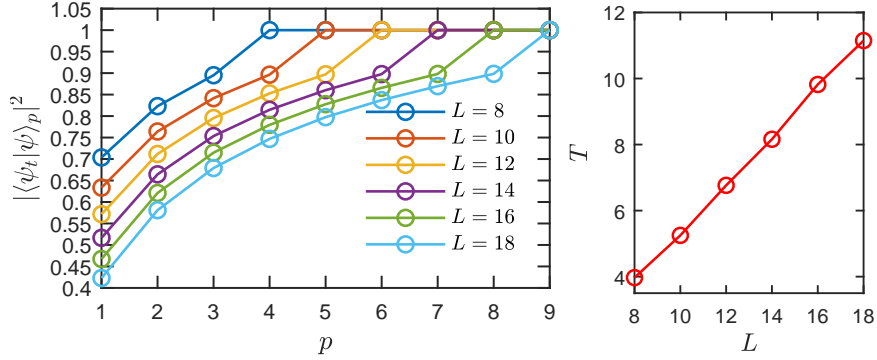


Figure 3: Preparation of critical state. (Left) Many-body overlap $|\langle \psi_t | \psi \rangle_p|^2$ of the prepared state with the target ground state of (5) found by exact diagonalization. One sees perfect fidelity for $p \geq L/2$. (Right) Total minimum time $T = \min_{(\gamma, \beta)} \left[\sum_{i=1}^{p=L/2} (\gamma_i + \beta_i) \right]$ required for the QAOA to produce the critical state with perfect fidelity using $\text{QAOA}_{p=L/2}$. One sees a linear trend $T \sim L$.

4.2 Critical state

Let us also consider the preparation of a critical state, namely the ground state of the 1d transverse field Ising model (TFIM) on a ring,

$$H_{\text{TFIM}} = - \sum_{i=1}^L Z_i Z_{i+1} - \sum_{i=1}^L X_i. \quad (5)$$

We use a variant of the QAOA scheme: we employ the protocol (2) with H_I still given by (4), but instead minimize the cost function (3) with H_{TFIM} in place of H_I . To benchmark the algorithm, we compute the many-body overlap $|\langle \psi_t | \psi \rangle_p|^2$ of the prepared state $|\psi\rangle_p$ with the corresponding target state $|\psi_t\rangle$ (the ground state of (5), obtained by exact diagonalization).

Figs. 3 show the results (see [41] for energy optimization plots and explicit optimal angles). Surprisingly, the critical state $|\psi_t\rangle$ can also be prepared with *perfect* fidelity to machine precision using QAOA_{p^*} , with $p^* = L/2$. This implies once again that the time t needed to prepare a critical state of this system of size L , exactly, goes as $t = O(L)$; we find additionally numerically that the minimum time T required scales linearly with the system size as $T \sim L$.

The perfect fidelities achieved for both the GHZ and critical cases suggest that an analytic understanding may be possible. However, while the model and unitary gates can be mapped to free fermions [44], the QAOA algorithm maps to a nonlinear optimization problem involving an extensive number of variables, which is highly nontrivial. In fact, we conjecture that, for a one-dimensional system of even L spin-1/2s with periodic boundary conditions, any state produced by QAOA_p for arbitrary p using $H_I = - \sum_{i=1}^L Z_i Z_{i+1}$ and $H_X = - \sum_{i=1}^L X_i$, can also be achieved perfectly by $\text{QAOA}_{p=L/2}$. This would imply that we can achieve the ground state of the TFIM at *any* point in the phase diagram using $\text{QAOA}_{p=L/2}$, which in particular would cover the GHZ and critical cases. In [41], we provide extra details and numerical evidence to support this conjecture.

4.3 Ground state of the Toric code

We next consider the preparation of a topologically ordered state, specifically the ground state of the \mathbb{Z}_2 Wen-plaquette model, which is unitarily equivalent to the Kitaev toric code:

$$H_I = - \sum_{i=1}^L \sum_{j=1}^L \sigma_{i,j+1}^x \sigma_{i+1,j+1}^y \sigma_{i+1,j}^x \sigma_{i,j}^y, \quad (6)$$

where we have written the Pauli matrices (X, Y, Z) as $(\sigma^x, \sigma^y, \sigma^z)$ and assumed periodic boundary conditions with even L . We find that there exists a QAOA protocol of $p = L/2$ iterations which perfectly prepares the ground state of (6).

The result can be understood from a map between the original σ spin variables and a dual set of spin variables τ s residing on the centers of plaquettes, which map the Wen plaquette model to decoupled chains of Ising models living on the diagonals. Concretely, let \mathcal{H}_S be the Hilbert space subject to the L constraints $\prod_{i=1}^L \sigma_{i,j}^x = 1$ for $j = 1, \dots, L$, which is conserved under time evolution by H_I and $H_X = - \sum_{i,j} \sigma_{i,j}^x$, which has $\dim \mathcal{H}_S = 2^{L^2-L}$. We now define a new set of Pauli operators τ residing on the centers of plaquettes (see also [45]); $\tau_{i,j}$ is located on the center of the plaquette with lower left corner at (i, j) . All operators preserving \mathcal{H}_S can be rewritten in terms of τ via:

$$\begin{aligned} \tau_{i,j}^x &= \sigma_{i,j+1}^x \sigma_{i+1,j+1}^y \sigma_{i+1,j}^x \sigma_{i,j}^y, \\ \tau_{i,j}^z \tau_{i+1,j+1}^z &= \sigma_{i+1,j+1}^x, \end{aligned} \quad (7)$$

subject to the L constraints $\prod_{i=1}^L \tau_{i,j}^x = 1$ for $j = 1, \dots, L$.

As the goal is to transform the trivial product state stabilized by $H_X = - \sum_{i=1}^L \sum_{j=1}^L \sigma_{i,j}^x$ to the topologically ordered state stabilized by H_I and the two logical operators $L_1 = \prod_{i=1}^L \sigma_{i,i}^x$ and $L_2 = \prod_{i=1}^L \sigma_{i,i+1}^x$, this is equivalent in the dual language to transforming the state stabilized by

$$\{-\tau_{i,j}^z \tau_{i+1,j+1}^z = -\sigma_{i+1,j+1}^x\}_{i=1}^L \quad (8)$$

and $\prod_{i=1}^L \tau_{i,j}^x = 1$, into the state stabilized by

$$\{-\tau_{i,j}^x = -\sigma_{i,j+1}^x \sigma_{i+1,j+1}^y \sigma_{i+1,j}^x \sigma_{i,j}^y\}_{i=1}^L, \quad (9)$$

i.e. converting the GHZ state defined on each diagonal (labeled j) of τ spins, to the trivial product state $\otimes_i |+\rangle_i$. Since there exists a circuit corresponding to $\text{QAOA}_{p=L/2}$ that prepares the GHZ state (shown earlier), the inverse of the circuit can be applied onto each diagonal of τ spins to achieve this result. In fact, since operators between diagonals commute, the circuit on each diagonal can in fact be done in parallel, i.e. a global evolution, and the ground state of the toric code prepared. Moreover, the logical operator (L_1, L_2) constraints are preserved at all steps (see [41] for a numerical illustration). The total minimum runtime T needed to implement this protocol, as found earlier, scales as $T \sim L$, which we note is a lower bound derived in [39].

4.4 Ground state of AFM Heisenberg chain

Lastly, we consider targeting the ground states of the AFM spin-1/2 Heisenberg chains with open boundary conditions,

$$H_I = \sum_{i=1}^{L-1} \mathbf{S}_i \cdot \mathbf{S}_{i+1}. \quad (10)$$

Instead of time evolving by alternating between H_I and H_X as before, we use a modified QAOA protocol: we start off with an easily preparable state comprised of disjoint products of Bell pairs: $\otimes_i \frac{1}{\sqrt{2}}(|\uparrow\downarrow\rangle - |\downarrow\uparrow\rangle)_{2i-1,2i}$, and sequentially time evolve it using two interaction Hamiltonians $H_1 = \sum_{i=1}^{L/2-1} \mathbf{S}_{2i} \cdot \mathbf{S}_{2i+1}$ and $H_2 = \sum_{i=1}^{L/2} \mathbf{S}_{2i-1} \cdot \mathbf{S}_{2i}$, whilst evaluating the expectation value of (10), i.e. the energy, as the cost function. Note that the angles can be restricted to $\gamma, \beta \in [0, 2\pi)$.

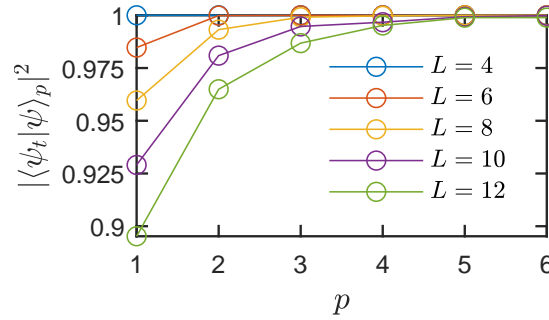


Figure 4: Fidelities in the preparation of ground states of AFM spin-1/2 Heisenberg chains of various sizes using QAOA.

Fig. 4 shows the results of the resulting fidelities, for various L s. We see that in this case, while the preparation of the ground states is generically not perfect at any finite p , the many-body fidelities are already very good for very low p s, at least for small system sizes, (e.g. $\sim 90\%$ at $L=12$ and $p=1$). This illustrates the utility and generality of QAOA in preparing non-trivial quantum states.

5 Conclusion

We have presented a general, efficient approach for preparing non-trivial quantum states based on QAOA, and demonstrated numerically its efficacy in the preparation of a number of target states of interest. The main merits of this approach are its practicality for quantum simulators and its ability to improve based on feedback from the simulator. The only two requirements—time evolution by two simple Hamiltonians—are realizable in synthetic quantum systems such as trapped ions and superconducting qubits. While in our examples considered we have chiefly focused on fixed point wavefunctions of certain non-trivial phases of matter described by integrable systems, we expect that the QAOA can efficiently accommodate targeting more general ground states of interacting Hamiltonians. An important question we

have also addressed in [41] is the effect of imperfect sequences on state preparation (such as noise); we have found that the resulting infidelities in the cases studied are reasonably small for near-term simulators, and these can be further decreased using feedback.

With the ability to efficiently prepare non-trivial quantum states, various studies are possible. Their non-trivial entanglement structure could be directly measured by preparing multiple copies of the states and using recently developed protocols [46, 47]; it would be interesting to extract the central charge of the critical system or topological entanglement entropy of the toric code state. Furthermore, truncating the analytic circuit at intermediate depth allows one to prepare a state with a boundary separating toric code and a trivial paramagnet.

More generally, in addition to providing practical circuits and variational wavefunctions, the QAOA is a potential tool for addressing questions of complexity of a ground state. In the examples provided, it furnishes circuits with minimal depth scaling with size and may offer valuable guidance in determining the circuit complexity [48–50] needed to prepare various states of matter.

Acknowledgements

We thank Daniel Gottesman, Gábor Halász, Germán Sierra, Romain Vasseur, Soonwon Choi, Shengtao Wang, Valentin Kasper, Sonika Johri and Karan Mehta for useful discussions.

Funding information WWH and THH are supported by the Moore Foundation’s EPIQS Initiative through Grant No. GBMF4306 and Grant No. GBMF4304 respectively.

A Optimal angles for preparing GHZ state at $p = L/2$

The following are the numerically found optimized set of angles $(\gamma_1, \beta_1, \dots, \gamma_{p=L/2}, \beta_{p=L/2})$ employed by $\text{QAOA}_{p=L/2}$ which produce the GHZ state with perfect fidelity at various system sizes and with least amount of time $T = \sum_i^{p=L/2} (\gamma_i + \beta_i)$.

$L = 8, T = 4.7867$:

$$(0.5297, 0.5243, 0.7243, 0.6151, 0.6151, 0.7243, 0.5243, 0.5297) \quad (11)$$

$L = 10, T = 6.257$:

$$(0.5814, 0.5230, 0.6360, 0.7889, 0.5993, 0.5993, 0.7889, 0.6360, 0.5230, 0.5814) \quad (12)$$

$L = 12, T = 7.651$:

$$\begin{aligned} &(0.5466, 0.5452, 0.6902, 0.7212, 0.5946, 0.7276 \\ &0.7276, 0.5946, 0.7212, 0.6902, 0.5452, 0.5466) \end{aligned} \quad (13)$$

$L = 14, T = 9.2634$:

$$\begin{aligned} &(0.6513, 0.5696, 0.5841, 0.6704, 0.7633, 0.8270, 0.5660, \\ &0.5660, 0.8270, 0.7633, 0.6704, 0.5841, 0.5696, 0.6513) \end{aligned} \quad (14)$$

$L = 16, T = 10.6273$:

$$(0.5846, 0.5796, 0.6105, 0.7155, , 0.7966, 0.6152, 0.6373, 0.7745, \\ 0.7745, 0.6373, 0.6152, 0.7966, 0.7155, 0.6105, 0.5796, 0.5846) \quad (15)$$

$L = 18, T = 12.096$:

$$(0.6064, 0.5232, 0.6632, 0.7780, 0.6660, 0.6302, 0.7773, 0.7133, 0.6904, \\ 0.6904, 0.7133, 0.7773, 0.6302, 0.6660, 0.7780, 0.6632, 0.5232, 0.6064) \quad (16)$$

B Explicit nonuniform unitary circuit for preparing the GHZ state

We provide here an analytic example of a unitary circuit that prepares exactly the GHZ state from the product state $|+\rangle$, complementary to the QAOA scheme, which highlights the Kramers-Wannier duality. This involves a nonuniform application of various 1-site and 2-site unitary gates. We first rewrite the spin degrees of freedom in terms of Majorana fermions, via the Jordan-Wigner transformation: $\gamma_{2j-1} = Y_j \prod_{i=1}^{j-1} X_i$, $\gamma_{2j} = Z_j \prod_{i=1}^{j-1} X_i$ for j ranging from 1 to L . Then $X_j = -i\gamma_{2j-1}\gamma_{2j}$ and $Z_j Z_{j+1} = i\gamma_{2j}\gamma_{2j+1}$; the product state and GHZ state thus simply correspond to the two different dimerization patterns of Majoranas. To transform from the state with all $i\gamma_{2j-1}\gamma_{2j} = -1$ to the state with all $i\gamma_{2j}\gamma_{2j+1} = +1$, we need to sequentially exchange Majoranas pairwise ($\gamma_1 \leftrightarrow \gamma_2, \gamma_2 \leftrightarrow \gamma_3, \dots$). $S = e^{\frac{i\pi}{4}i\gamma_i\gamma_j}$ is the SWAP operator which accomplishes each exchange: $S^{-1}\gamma_{i,j}S = \mp\gamma_{j,i}$. Thus, U is a product of successive SWAPs, which in the spin language is

$$U = \left(\prod_{i=1}^{L-1} e^{\frac{i\pi}{4}X_{i+1}} e^{\frac{i\pi}{4}Z_i Z_{i+1}} \right) e^{\frac{i\pi}{4}X_1}. \quad (17)$$

As the last operator (when acting on $\otimes|X = 1\rangle$) contributes an overall phase and can be neglected, we have analytically found a depth $2(L-1)$ circuit relating GHZ and product states exactly; this complements the QAOA circuit discussed earlier. We note that such SWAPs were also used in [51] to transform a product state into the ground state of the Kitaev chain, .

C Energy optimization plot and optimal angles for preparing critical state at $p = L/2$

In Fig. 5 we present the optimal cost function given by the energy of the TFIM,

$$F_p(\gamma, \beta) = {}_p\langle \psi(\gamma, \beta) | H_{\text{TFIM}} | \psi(\gamma, \beta) \rangle_p, \quad (18)$$

used in the preparation of the critical state.

The following are the numerically found optimized set of angles $(\gamma_1, \beta_1, \dots, \gamma_{p=L/2}, \beta_{p=L/2})$ employed by QAOA $_{p=L/2}$ which produce the critical state with perfect fidelity at various system sizes and with least amount of time $T = \sum_i^{p=L/2} (\gamma_i + \beta_i)$.

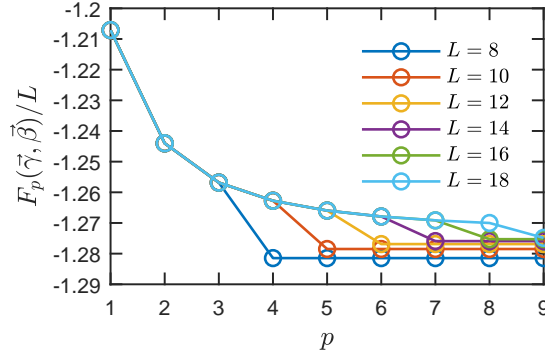


Figure 5: Preparation of critical state. Optimal cost function (18) with energy as measured by the TFIM Hamiltonian.

$L = 8, T = 3.9699 :$

$$(0.2496, 0.6845, 0.4808, 0.6559, 0.5260, 0.6048, 0.4503, 0.3180) \quad (19)$$

$L = 10, T = 5.250:$

$$(0.2473, 0.6977, 0.4888, 0.6783, 0.5559, 0.6567, 0.5558, 0.6029, 0.4598, 0.3068) \quad (20)$$

$L = 12, T = 6.7651:$

$$(0.2809, 0.6131, 0.6633, 0.4537, 0.8653, 0.4663, \\ 0.6970, 0.6829, 0.4569, 0.7990, 0.3565, 0.4304) \quad (21)$$

$L = 14, T = 8.1604:$

$$(0.3090, 0.5710, 0.6923, 0.5648, 0.5391, 0.9684, 0.3979, \\ 0.6852, 0.8235, 0.4474, 0.6930, 0.6465, 0.4120, 0.4104) \quad (22)$$

$L = 16, T = 9.8198:$

$$(0.3790, 0.5622, 0.5638, 0.7101, 0.9046, 0.3210, 0.6738, 0.8377, \\ 0.8616, 0.4004, 0.5624, 0.9450, 0.5224, 0.6466, 0.4119, 0.5172) \quad (23)$$

$L = 18, T = 11.1485:$

$$(0.3830, 0.4931, 0.7099, 0.7010, 0.5330, 0.6523, 0.6887, 1.0405, 0.3083, \\ 0.6215, 0.9607, 0.5977, 0.6209, 0.5597, 0.7850, 0.5851, 0.4132, 0.4948) \quad (24)$$

D A Conjecture and Numerical Support

Consider a one-dimensional system of an even number L spin-1/2s with periodic boundary conditions, and consider $H_I = -\sum_{i=1}^L Z_i Z_{i+1}$ and $H_X = -\sum_i X_i$. Our conjecture is that

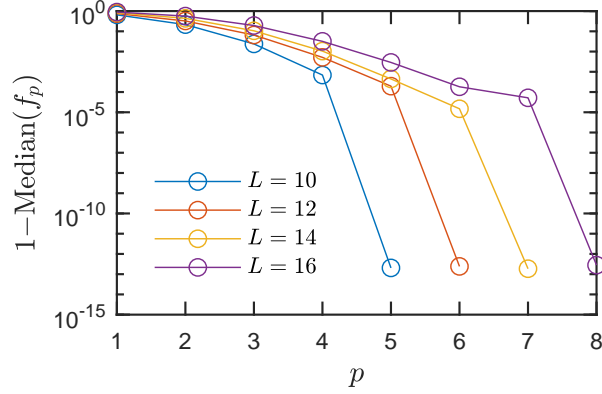


Figure 6: Typical optimal infidelity of QAOA_p for $1 \leq p \leq L/2$ used to target a random state produced by $\text{QAOA}_{p=L/2+1}$ (given by the median over 5000 realizations of random states). One sees a clear dip at $p = L/2$, to a value close to machine precision (which we take to be $\sim 10^{-13}$), indicating that the $\text{QAOA}_{p=L/2}$ is able to target a random state with perfect fidelity typically.

any state produced by a QAOA_p protocol of arbitrary p can be obtained by $\text{QAOA}_{p=L/2}$. In other words, for any p and set of angles $(\gamma, \beta) \equiv (\gamma_1, \dots, \gamma_p, \beta_1, \dots, \beta_p)$, there exists a set of angles $(\gamma', \beta') \equiv (\gamma'_1, \dots, \gamma'_{L/2}, \beta'_1, \dots, \beta'_{L/2})$ such that

$$e^{-i\beta'_{L/2}H_X} e^{-i\gamma'_{L/2}H_I} \dots e^{-i\beta'_1H_X} e^{-i\gamma'_1H_I} |+\rangle \quad (25)$$

$$= e^{-i\beta_pH_X} e^{-i\gamma_pH_I} \dots e^{-i\beta_1H_X} e^{-i\gamma_1H_I} |+\rangle. \quad (26)$$

It suffices to establish this result for $p = L/2 + 1$, because one could then contract the $p = (L/2 + 1)$ QAOA unitary into a $p = L/2$ QAOA unitary, and iterate this process to achieve finally a $p = L/2$ QAOA unitary. We have tested this result for different system sizes by generating random states $|\psi^{(r)}(\gamma, \beta)\rangle_{L/2+1}$ produced using the $\text{QAOA}_{p=L/2+1}$ protocol with random angles $(\gamma_1, \dots, \gamma_{L/2+1}, \beta_1, \dots, \beta_{L/2+1})$, and targeting them using the protocol QAOA_p for p up to $L/2$. More precisely, given a random state $|\psi^{(r)}(\gamma, \beta)\rangle_{L/2+1}$, we maximize the fidelity

$$f_p(\gamma', \beta') = \left| {}_p\langle \psi(\gamma', \beta') | \psi^{(r)}(\gamma, \beta) \rangle_{L/2+1} \right|^2, \quad (27)$$

over (γ', β') , where $|\psi(\gamma', \beta')\rangle_p$ is the state produced by QAOA_p .

Figs. 6, 7 show the results. In fig. 6, we plot the typical optimal infidelity $1 - \text{Median}(f_p)$, given by the median over all realizations of random states (we have used 5000 random states and ensured convergence of the algorithm to the global minimum) against p , and for various L s. We see that a typical run of QAOA_p for $p = L/2$ is able to target the input state $|\psi^{(r)}(\gamma, \beta)\rangle_{L/2+1}$ with perfect fidelity (to machine precision), while not for $p < L/2$. The reason we do not use the mean value, is because this undesirably overly weights the contributions of numerical imprecisions in the optimization algorithm. However, to make a statement about whether $\text{QAOA}_{p=L/2}$ is able to *always* reach the target random state, we need to analyze the

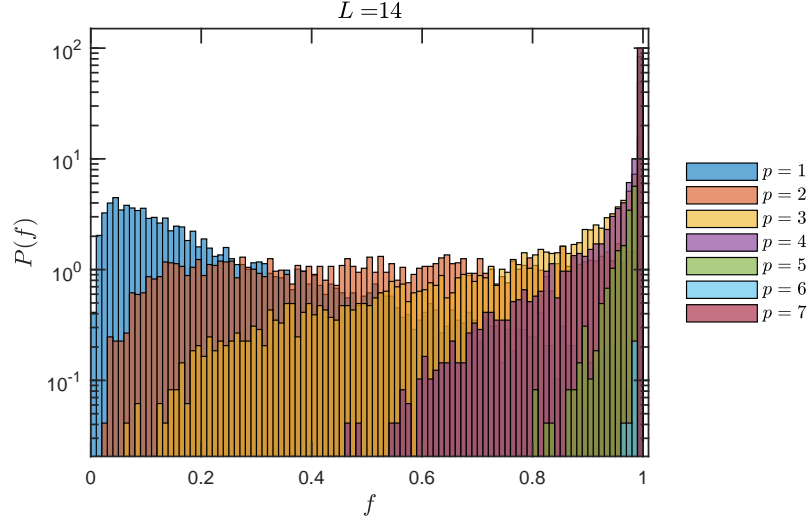


Figure 7: Probability distribution of optimal fidelities, for system size $L = 14$. For $p = L/2$, the optimal fidelities are singularly peaked at $f = 1$, indicating that *all* instances of random states produced by $\text{QAOA}_{p=L/2+1}$ can be targeted using $\text{QAOA}_{p=L/2}$ perfectly; this is in contrast to $p < L/2$ where there is some spread in the distribution, indicating that there are instances of random states for which $\text{QAOA}_{p < L/2}$ cannot target them. Probability distributions for other system sizes is qualitatively similar to one shown here.

full *distribution* of the optimal fidelities. In fig. 7, we plot the *distribution* of the optimal fidelities for one of the system sizes considered and for various p s by plotting the probability distributions $P(f)$ of the optimal fidelities f . We find that at $p = L/2$, the distribution is singularly peaked at $f = 1$ (to machine precision), indicating that in fact, *all* realizations of random states created using $\text{QAOA}_{p=L/2+1}$ can be targeted with $\text{QAOA}_{p=L/2}$, perfectly. This is in contrast to the optimal fidelities obtained for $p < L/2$: there is some spread in the distributions, indicating that there are instances of random states for which $\text{QAOA}_{p < L/2}$ cannot reproduce it. Thus, our numerics gives support to the conjecture that any state produced using $\text{QAOA}_{p \geq L/2+1}$ can be obtained by $\text{QAOA}_{p=L/2}$.

One important consequence of the above conjecture is that the ground state of any point in the transverse field Ising model ($H = H_I + gH_X$ for arbitrary g) can be achieved with perfect fidelity by $\text{QAOA}_{p=L/2}$. This is because as the number of iterations p approaches infinity, QAOA includes the trotterized adiabatic algorithm as a subset, and the latter can achieve any ground state in the phase diagram if infinite depth is permitted. Our conjecture then implies that such a circuit can be contracted to one with $p = L/2$.

As for proving the conjecture, we note that that leveraging the free fermion representation of the model, as done in [44], is a promising route. However, such a representation nonetheless involves a nonlinear (and hence nontrivial) optimization problem which we leave for future work.

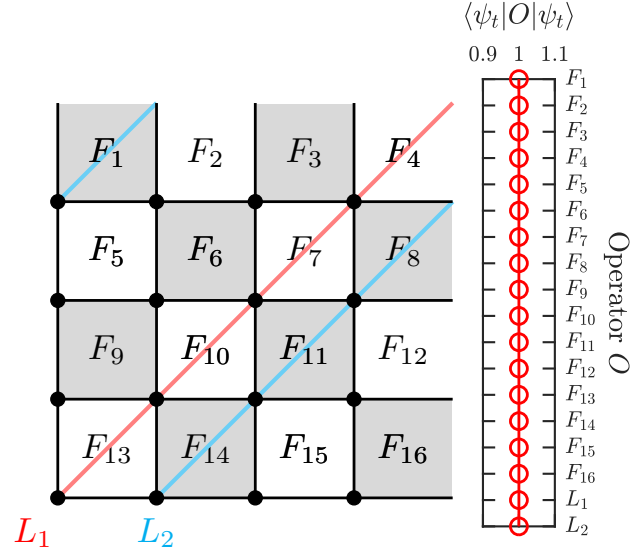


Figure 8: Numerical preparation the of Wen plaquette ground state using $\text{QAOA}_{p=L/2}$. Here $L = 4$, and we use the angles found from QAOA_2 that produced the GHZ state. The left plot describes the geometry of the set-up, and illustrate the plaquette operators F_i which make up the Hamiltonian $H = -\sum_i F_i$ as well as the two logical operators L_1 and L_2 which wrap around the torus. The right plot shows the expectation value of the plaquette operators and logical operators in the state prepared by QAOA. One sees that all expectation values are +1 to machine precision, indicating a perfect preparation of the ground state.

E Numerical verification of preparation of toric code ground state

We show here numerics that verify that we can prepare using $\text{QAOA}_{p=L/2}$ the ground state of the Wen-plaquette model in the sector $(L_1, L_2) = (+1, +1)$, using the angles found previously of a $\text{QAOA}_{p=L/2}$ circuit which prepared the GHZ state. Fig. 8 shows the result for a $L \times L$ Wen-plaquette model, where $L = 4$ (so that there are only four angles $(\gamma_1, \gamma_2, \beta_1, \beta_2)$ employed by the QAOA protocol). We see that all plaquette operators and logical operators carry a unit expectation value in the state prepared by the QAOA, which indicates that we can indeed prepare the ground state of the Wen-plaquette model in the appropriate logical sector as mentioned in the main text.

Note that this circuit derived from QAOA is different from the analytic depth- $2(L-1)$ circuit (using SWAP operators) that also prepares the Wen-plaquette ground state exactly.

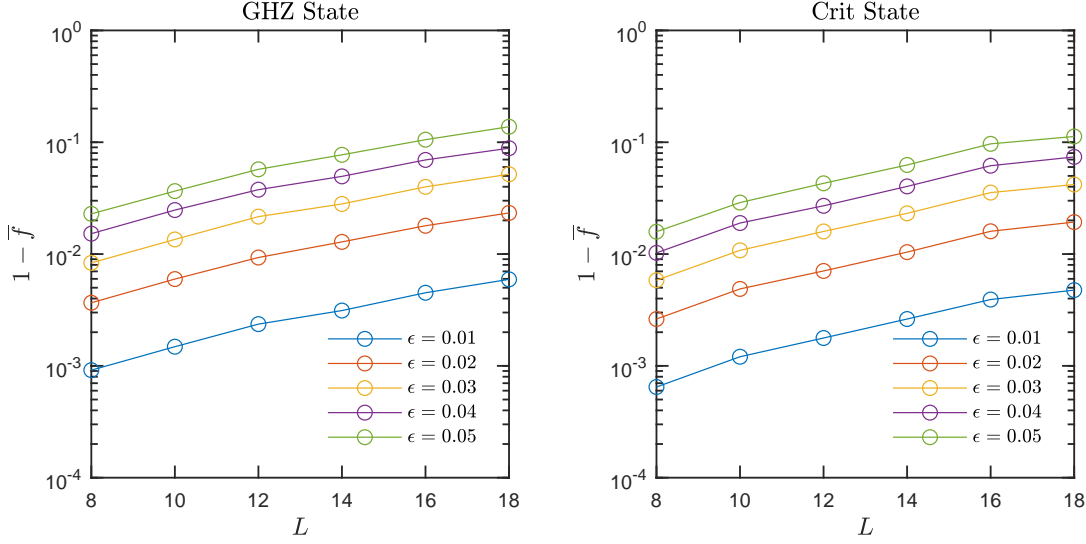


Figure 9: Effect of errors of strength ϵ on the QAOA preparation of GHZ and critical states for system size L . Plotted is the infidelity averaged over 1000 error realizations (denoted by the overline).

F Effect of errors on QAOA state preparation

To probe the sensitivity of our state preparation protocol to imperfections, we introduced random errors to the optimal angles and calculated the resulting infidelity $f = 1 - |\langle \psi_t | \psi \rangle|_{L/2}^2$ for QAOA $_{p=L/2}$, averaged over 1000 realizations of errors. Specifically, for each optimal angle γ_* , we introduce an error $\gamma = \gamma_*(1 + \epsilon R)$, where R is chosen randomly from the uniform distribution $[-1, 1]$ and ϵ parameterizes the strength of error (0.01, 0.02, 0.03, 0.04, or 0.05 in our study).

Fig. 9 shows the results for both the GHZ and critical states, for various system sizes and error strengths. Although the infidelity appears to increase exponentially with L , we see that for experimentally accessible system sizes (on the order of ten qubits), the infidelity is small (< 0.01 infidelity for $\epsilon = 0.01$ in $L = 18$).

References

- [1] R. Blatt and C. F. Roos, Quantum simulations with trapped ions, *Nature Physics* **8**, 277 (2012).
- [2] J. Zhang, G. Pagano, P. W. Hess, A. Kyprianidis, P. Becker, H. Kaplan, A. V. Gorshkov, Z.-X. Gong and C. Monroe, Observation of a many-body dynamical phase transition with a 53-qubit quantum simulator, *Nature* **551**, 601 EP (2017).
- [3] I. Bloch, J. Dalibard and W. Zwerger, Many-body physics with ultracold gases, *Rev. Mod. Phys.* **80**, 885 (2008), doi:10.1103/RevModPhys.80.885.

- [4] H. Bernien, S. Schwartz, A. Keesling, H. Levine, A. Omran, H. Pichler, S. Choi, A. S. Zibrov, M. Endres, M. Greiner, V. Vuletic and M. D. Lukin, Probing many-body dynamics on a 51-atom quantum simulator, Nature **551**, 579 EP (2017), Article.
- [5] R. Barends, J. Kelly, A. Megrant, D. Sank, E. Jeffrey, Y. Chen, Y. Yin, B. Chiaro, J. Mutus, C. Neill, P. O'Malley, P. Roushan et al., Coherent josephson qubit suitable for scalable quantum integrated circuits, Phys. Rev. Lett. **111**, 080502 (2013), doi:10.1103/PhysRevLett.111.080502.
- [6] J. M. Gambetta, J. M. Chow and M. Steffen, Building logical qubits in a superconducting quantum computing system, npj Quantum Information **3**(1), 2 (2017), doi:10.1038/s41534-016-0004-0.
- [7] M. Aidelsburger, M. Atala, M. Lohse, J. T. Barreiro, B. Paredes and I. Bloch, Realization of the hofstadter hamiltonian with ultracold atoms in optical lattices, Phys. Rev. Lett. **111**, 185301 (2013), doi:10.1103/PhysRevLett.111.185301.
- [8] G. Jotzu, M. Messer, R. Desbuquois, M. Lebrat, T. Uehlinger, D. Greif and T. Esslinger, Experimental realization of the topological haldane model with ultracold fermions, Nature **515**, 237 EP (2014).
- [9] M. Aidelsburger, M. Lohse, C. Schweizer, M. Atala, J. Barreiro, S. Nascimbène, N. R. Cooper, I. Bloch and N. Goldman, Measuring the chern number of hofstadter bands with ultracold bosonic atoms, Nature Physics **11**, 162 EP (2014).
- [10] M. Greiner, O. Mandel, T. Esslinger, T. W. Hänsch and I. Bloch, Quantum phase transition from a superfluid to a mott insulator in a gas of ultracold atoms, Nature **415**, 39 EP (2002), Article.
- [11] J.-y. Choi, S. Hild, J. Zeiher, P. Schauß, A. Rubio-Abadal, T. Yefsah, V. Khemani, D. A. Huse, I. Bloch and C. Gross, Exploring the many-body localization transition in two dimensions, Science **352**(6293), 1547 (2016), doi:10.1126/science.aaf8834.
- [12] M. Schreiber, S. S. Hodgman, P. Bordia, H. P. Lüschen, M. H. Fischer, R. Vosk, E. Altman, U. Schneider and I. Bloch, Observation of many-body localization of interacting fermions in a quasirandom optical lattice, Science **349**(6250), 842 (2015), doi:10.1126/science.aaa7432.
- [13] G. Kucsko, S. Choi, J. Choi, P. C. Maurer, H. Sumiya, S. Onoda, J. Isoya, F. Jelezko, E. Demler, N. Y. Yao and M. D. Lukin, Critical thermalization of a disordered dipolar spin system in diamond, ArXiv e-prints (2016), 1609.08216.
- [14] J. Zhang, P. W. Hess, A. Kyprianidis, P. Becker, A. Lee, J. Smith, G. Pagano, I.-D. Potirniche, A. C. Potter, A. Vishwanath, N. Y. Yao and C. Monroe, Observation of a discrete time crystal, Nature **543**(7644), 217 (2017).
- [15] S. Choi, J. Choi, R. Landig, G. Kucsko, H. Zhou, J. Isoya, F. Jelezko, S. Onoda, H. Sumiya, V. Khemani, C. von Keyserlingk, N. Y. Yao et al., Observation of discrete time-crystalline order in a disordered dipolar many-body system, Nature **543**(7644), 221 (2017).

- [16] J. Smith, A. Lee, P. Richerme, B. Neyenhuis, P. W. Hess, P. Hauke, M. Heyl, D. A. Huse and C. Monroe, Many-body localization in a quantum simulator with programmable random disorder, *Nature Physics* **12**, 907 EP (2016).
- [17] D. Leibfried, M. D. Barrett, T. Schaetz, J. Britton, J. Chiaverini, W. M. Itano, J. D. Jost, C. Langer and D. J. Wineland, Toward heisenberg-limited spectroscopy with multiparticle entangled states, *Science* **304**(5676), 1476 (2004), doi:10.1126/science.1097576.
- [18] V. Giovannetti, S. Lloyd and L. Maccone, Quantum-enhanced measurements: Beating the standard quantum limit, *Science* **306**(5700), 1330 (2004), doi:10.1126/science.1104149.
- [19] C. L. Degen, F. Reinhard and P. Cappellaro, Quantum sensing, *Rev. Mod. Phys.* **89**, 035002 (2017), doi:10.1103/RevModPhys.89.035002.
- [20] S. Choi, N. Y. Yao and M. D. Lukin, Quantum metrology based on strongly correlated matter, *ArXiv e-prints* (2018), 1801.00042.
- [21] R. Raussendorf, D. E. Browne and H. J. Briegel, Measurement-based quantum computation on cluster states, *Phys. Rev. A* **68**, 022312 (2003), doi:10.1103/PhysRevA.68.022312.
- [22] H. J. Briegel, D. E. Browne, W. Dür, R. Raussendorf and M. Van den Nest, Measurement-based quantum computation, *Nature Physics* **5**, 19 EP (2009).
- [23] B. P. Lanyon, P. Jurcevic, M. Zwerger, C. Hempel, E. A. Martinez, W. Dür, H. J. Briegel, R. Blatt and C. F. Roos, Measurement-based quantum computation with trapped ions, *Phys. Rev. Lett.* **111**, 210501 (2013), doi:10.1103/PhysRevLett.111.210501.
- [24] E. Farhi, J. Goldstone and S. Gutmann, A Quantum Approximate Optimization Algorithm, *ArXiv e-prints* (2014), 1411.4028.
- [25] E. Farhi and A. W. Harrow, Quantum Supremacy through the Quantum Approximate Optimization Algorithm, *ArXiv e-prints* (2016), 1602.07674.
- [26] E. Farhi, J. Goldstone, S. Gutmann and M. Sipser, Quantum Computation by Adiabatic Evolution, eprint arXiv:quant-ph/0001106 (2000), quant-ph/0001106.
- [27] E. Farhi, J. Goldstone, S. Gutmann, J. Lapan, A. Lundgren and D. Preda, A quantum adiabatic evolution algorithm applied to random instances of an np-complete problem, *Science* **292**(5516), 472 (2001), doi:10.1126/science.1057726.
- [28] K. Agarwal, R. N. Bhatt and S. L. Sondhi, Fast preparation of critical ground states using superluminal flow, *ArXiv e-prints* (2017), 1710.09840.
- [29] L. Pontryagin, Mathematical Theory of Optimal Processes (1987).
- [30] R. F. Stengel, Optimal Control and Estimation (1994).
- [31] C. Brif, M. D. Grace, M. Sarovar and K. C. Young, Exploring adiabatic quantum trajectories via optimal control, *New Journal of Physics* **16**(6), 065013 (2014).

- [32] Z.-C. Yang, A. Rahmani, A. Shabani, H. Neven and C. Chamon, Optimizing variational quantum algorithms using pontryagin’s minimum principle, Phys. Rev. X **7**, 021027 (2017), doi:10.1103/PhysRevX.7.021027.
- [33] F. Verstraete, J. I. Cirac and J. I. Latorre, Quantum circuits for strongly correlated quantum systems, Phys. Rev. A **79**, 032316 (2009), doi:10.1103/PhysRevA.79.032316.
- [34] M. Aguado and G. Vidal, Entanglement renormalization and topological order, Phys. Rev. Lett. **100**, 070404 (2008), doi:10.1103/PhysRevLett.100.070404.
- [35] J. Preskill, Quantum Computing in the NISQ era and beyond, Quantum **2**, 79 (2018), doi:10.22331/q-2018-08-06-79.
- [36] M. B. Hastings, Locality in Quantum Systems, ArXiv e-prints (2010), 1008.5137.
- [37] A. Kitaev and J. Preskill, Topological entanglement entropy, Phys. Rev. Lett. **96**, 110404 (2006), doi:10.1103/PhysRevLett.96.110404.
- [38] M. Levin and X.-G. Wen, Detecting topological order in a ground state wave function, Phys. Rev. Lett. **96**, 110405 (2006), doi:10.1103/PhysRevLett.96.110405.
- [39] S. Bravyi, M. B. Hastings and F. Verstraete, Lieb-robinson bounds and the generation of correlations and topological quantum order, Phys. Rev. Lett. **97**, 050401 (2006), doi:10.1103/PhysRevLett.97.050401.
- [40] C.-M. Jian, I. Kim and X.-L. Qi, Long-range mutual information and topological uncertainty principle, ArXiv e-prints (2015), 1508.07006.
- [41] See supplemental information.
- [42] A. Sørensen and K. Mølmer, Entanglement and quantum computation with ions in thermal motion, Phys. Rev. A **62**, 022311 (2000), doi:10.1103/PhysRevA.62.022311.
- [43] T. Monz, P. Schindler, J. T. Barreiro, M. Chwalla, D. Nigg, W. A. Coish, M. Harlander, W. Hänsel, M. Hennrich and R. Blatt, 14-qubit entanglement: Creation and coherence, Phys. Rev. Lett. **106**, 130506 (2011), doi:10.1103/PhysRevLett.106.130506.
- [44] Z. Wang, S. Hadfield, Z. Jiang and E. G. Rieffel, Quantum approximate optimization algorithm for maxcut: A fermionic view, Phys. Rev. A **97**, 022304 (2018), doi:10.1103/PhysRevA.97.022304.
- [45] J. Yu, S.-P. Kou and X.-G. Wen, Topological quantum phase transition in the transverse wen-plaquette model, EPL (Europhysics Letters) **84**(1), 17004 (2008).
- [46] D. A. Abanin and E. Demler, Measuring entanglement entropy of a generic many-body system with a quantum switch, Phys. Rev. Lett. **109**, 020504 (2012), doi:10.1103/PhysRevLett.109.020504.
- [47] R. Islam, R. Ma, P. M. Preiss, M. Eric Tai, A. Lukin, M. Rispoli and M. Greiner, Measuring entanglement entropy in a quantum many-body system, Nature **528**, 77 EP (2015), Article.

- [48] M. A. Nielsen, A geometric approach to quantum circuit lower bounds, Quantum Info. Comput. **6**(3), 213 (2006).
- [49] L. Susskind, Entanglement is not enough, ArXiv e-prints (2014), 1411.0690.
- [50] R. A. Jefferson and R. C. Myers, Circuit complexity in quantum field theory, Journal of High Energy Physics **2017**(10), 107 (2017), doi:10.1007/JHEP10(2017)107.
- [51] Y. Huang and X. Chen, Quantum circuit complexity of one-dimensional topological phases, Phys. Rev. B **91**, 195143 (2015), doi:10.1103/PhysRevB.91.195143.